Journal of Engineering Sciences

Vol 13, Issue 06, June/2022

ISSN NO:0377-9254

A New Electric Vehicle Battery Charging Based Efficient Inductive Power Transfer Topology

ISUKAPALLI PAVAN KUMAR, J S SRINIVASA RAJU
M.Tech Student, Assistant Professor
Dept Of EEE
Universal college of engineering and technology, Dokiparru, Guntur, A.P 522005

Abstract—Recently available high-frequency power converter topologies for inductive power transfer (IPT) system utilize either zero voltage switching (ZVS) or zero current switching (ZCS) based power electronic converters while maintaining a near sinusoidal current for limited power transfer range. However, achieving ZVS or ZCS for all power switches simultaneously is still a challenging task in IPT systems. In this article, an improved zero-voltage zero-current switching (ZVZCS) IPT topology and its switching pattern are proposed. ZVS is achieved by optimizing the classical series compensation and additionally, an auxiliary network is employed to achieve ZCS. The proposed concept is verified by using MATLAB/Simulink based simulations for resistive and battery load. Finally, the practical viability of the proposed topology is validated by the results obtained using a laboratory prototype rated for 1.1 kW, 85 kHz. An efficiency of 91.26% is achieved with ZVZCS for a full dynamic power transfer range of 20 W–1.1 kW.

Index Terms—Battery chargers, dc–dc power converters, electric vehicles (EVs), inductive charging, soft switching, wireless power transmission.

I.INTRODUCTION

THE increasingly global economy is facing the demolition of fuel resources along with hazardous disturbances in environmental conditions. Moreover, it has spurred the emergence of sustainable technologies leading to innovations in major carbon contributors, i.e., transportation [1], [2]. Therefore, electric vehicles (EVs) are adopted as a solution to diminish the environmental effects caused by carbon-based fuels [2], [3]. Furthermore, the EVs market opens a new opportunity for human beings to expand the life expectancy of transportation at a lower cost [1], [3]. In the past, the battery technology (BT) and power shaping technologies are the limitations to put EVs out of market success. However, BT has been evolved with high energy density, lesser weight, and high efficiency in a few past decades [4]. Additionally, efficient energy storage device improves overall performance while used with a suitable power shaping circuit. A dc–dc power conditioning configuration having subservient power losses, durability, reliable energy transfer, and increased charging-discharging cycles are exercised by researchers and industries [1]–[4]. Nowadays, efficient, fast chargers are deployed for short driving range with human safety concerns. In the present scenario, the inductive power transfer (IPT)-based typologies are adopted as safer battery charging (BC) solutions during EV stationary and dynamic mode. Compensation networks are presented to crimp the circuit impedance for improving the overall efficiency of the converter. However, the number of active and passive elements of the circuits comprises with the complexity of the configuration [5].

The right solution further improves the driving range, maintenance cycle, reduced carbon footprint, and enduser economy. Therefore, converter selection plays a vital role in EV's flow in the market. Consequently, it supports decrement in environmental problems produced by transportation issues expertly [6]. The classical series-series capacitor compensation based IPT topology is one of the most preferred network arrangement adopted by industries because of its structure simplicity and operational stability for varying coils distance [7]. This network presents a low-cost solution but compromises its efficiency, power transfer capability, high resonant peaks, and control accuracy for variant loading.

In [7], an algorithm for phase control is presented to enhance efficiency bandwidth; however, the expense results as a sophisticated control strategy for variant frequency. In [8], issues generated by variable frequency are mitigated by defining the control boundary in the optimal frequency range. The control solutions presented in [7] and [8] only supports clam to provide higher efficiency by maintaining zero voltage switching (ZVS) for IPT system. The topological advancement in [9] has been done by a new coil support network using intermediate L–C series compensated structure at both the transmitter and receiver end. This configuration increases weight at the vehicle side, which is mitigated in [10], by placing both coils on the primary side. The solution presented in [9] and [10] provides magnetic flux support in misalignment condition but decreases the beauty of simplicity in calculation and control operation. A solution to the issues present in [9] and [10] as an isolated tank network to support IPT is addressed in [11] by incorporating an H-bridge high-frequency transformer with L–C tank network. However, it increases the size, weight, and volume of

the whole system while reducing peak efficiency. Therefore, a solution as the reconstruction of the passive component's network is presented in [12]–[17] to mitigate issues sprouted by an additional magnetically isolated resonant tank. In [12] and [13], a symmetrical filter network is cascaded with loosely coupled transformer coils to improve the performance of the system for a long duration. However, these topologies implement magnetically isolated inductors, which increase weight, volume, complexity in tuning method, and decrease efficiency. These issues are addressed in [14] and [15] by employing asymmetrical compensation using the LCC-C network configuration. The analysis of claims presented in [12]–[15] are comparatively studied in [16] and [17], and it is found that for the same coil design, LCC–LCC network is suitable for stationary IPT and LCC-C for dynamic IPT.

However, it suffers distortions in the case of vehicle side topology and clearance variations. Therefore, Zhang et al. [16] and Li et al. [17] direct to find a different solution utilizing series C–C compensation. In [18]–[20], a solution to stabilize soft switching for a wide operating range, improved efficiency, performance for the strongly coupled transformer-based dc–dc converter is presented. In [21] and [22], the auxiliary network is adopted to enhance the performance of resonant IPT topology based on [18]–[20]. The constant losses have been increased because of additional magnetics while stable operation with improved efficiency is obtained. Likewise, a solution for resonant IPT based series C–C compensated topology is presented in [23]. In this view point, IPT with auxiliary circuit can mitigate issues present in voltage source inverter (VSI) fed converter based network. In this article, the proposed topology utilizes classical series L–C compensation with a small size auxiliary components to make ZVS along with zero current switching (ZCS). The proposed topology offers a constant output voltage even if the input is subjected to a wide range of voltage variations. The output current can easily be controlled from the input side voltage, which eliminates the requirement of a high-power processor for controlling operation, and the cost for the converter is effectively reduced. A laboratory prototype has been developed and tested for resistive and battery load for full BC range. Fig. 1 shows the general overview of the proposed topology in which two stages of the converter have been controlled by using modified pulsewidth modulation (MPWM) separately. The pulses are generated at 85 kHz switching frequency in MPWM mode to achieve zero-voltage zero-current switching (ZVZCS) to deliver power up to 1.1 kW, and performance results are presented.

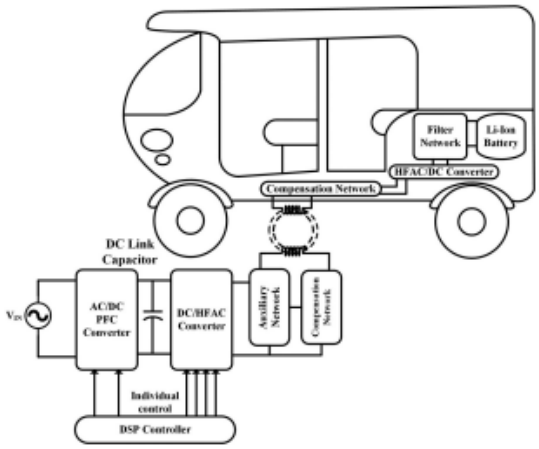

Fig. 1. General configuration of wireless battery charger topology

II.ELECTRIC VEHICLE

An **electric vehicle**, also called an **EV**, uses one or more electric motors or traction motors for propulsion. An electric vehicle may be powered through a collector system by electricity from off-vehicle sources, or may be self-contained with a battery, solar panels or an electric generator to convert fuel to electricity.[1] EVs include, but are not limited to, road and rail vehicles, surface and underwater vessels, electric aircraft and electric spacecraft.

EVs first came into existence in the mid-19th century, when electricity was among the preferred methods for motor vehicle propulsion, providing a level of comfort and ease of operation that could not be achieved by the gasoline cars of the time. Modern internal combustion engines have been the dominant propulsion method for motor vehicles for almost 100 years, but electric power has remained commonplace in other vehicle types, such as trains and smaller vehicles of all types.

In the 21st century, EVs saw a resurgence due to technological developments, and an increased focus on renewable energy. A great deal of demand for electric vehicles developed and a small core of do-it-yourself (DIY) engineers began sharing technical details for doing electric vehicle conversions. Government incentives to increase adoptions were introduced, including in the United States and the European Union

Journal of Engineering Sciences

Vol 13, Issue 06, June/2022

ISSN NO:0377-9254

Edison and a 1914 Detroit Electricmodel 47 (courtesy of the National Museum of American History)

An EV and an antique car on display at a 1912 auto show

II.POWER FACTOR

The electrical energy is almost exclusively generated, transmitted and distributed in the form of alternating current. Therefore, the question of power factor immediately comes into picture. Most of the loads (e.g. induction motors, arc lamps) are inductive in nature and hence have low lagging power factor. The low power factor is highly undesirable as it causes an increase in current, resulting in additional losses of active power in all the elements of power system from power station generator down to the utilisation devices. In order to ensure most favorable conditions for a supply system from engineering and economical standpoint, it is important to have power factor as close to unity as possible. In this chapter, we shall discuss the various methods of power factor improvement.

The cosine of angle between voltage and current in an a.c. circuit is known as power factor**.** In an a.c. circuit, there is generally a phase difference φ between voltage and current. The term cos φ is called the power factor of the circuit. If the circuit is inductive, the current lags behind the voltage and the power factor is referred to as lagging. However, in a capacitive circuit, current leads the voltage and power factor is said to be leading. Consider an inductive circuit taking a lagging current I from supply voltage V; the angle of lag being φ. The phasor diagram of the circuit is shown in Fig. 6.1.

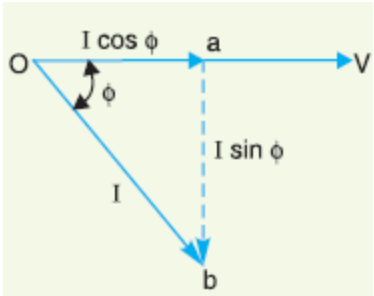

Fig. 6.1

The circuit current I can be resolved into two perpendicular components, namely ;
(a) I cos φ in phase with V
(b) I sin φ 90o out of phase with V

PULSE WIDTH MODULATION

Pulse Width Modulation (PWM) is the most effective means to achieve constant voltage battery charging by switching the solar system controller's power devices. When in PWM regulation, the current from the solar array tapers according to the battery's condition and recharging needs Consider a waveform such as this: it is a voltage switching between 0v and 12v. It is fairly obvious that, since the voltage is at 12v for exactly as long as it is at 0v, then a 'suitable device' connected to its output will see the average voltage and think it is being fed 6v - exactly half of 12v. So by varying the width of the positive pulse - we can vary the 'average' voltage.
Similarly, if the switches keep the voltage at 12 for 3

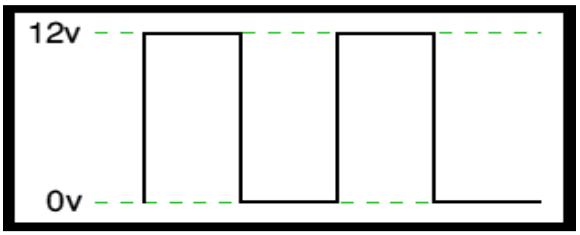

times as long as at 0v, the average will be 3/4 of 12v - or 9v, as shown below.

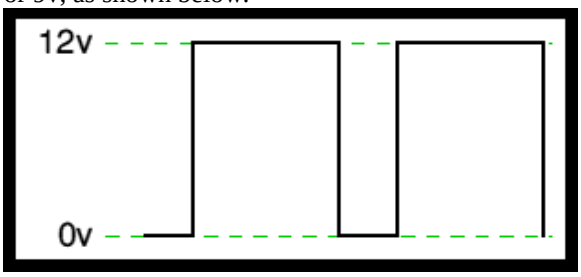

and if the output pulse of 12v lasts only 25% of the overall time, then the average is

IV.PROJECT DESCRIPTION AND CONTROL DESIGN

OPERATING PRINCIPLE OF THE PROPOSED CONVERTER

Active switches S1 − S4 at primary side and diodes D5 − D8 at secondary side forms a H-bridge (conventional). Moreover, Ca1 and Ca2 act as potential divider at the input with ancillaryLA and TA to maintain the soft-switching feature of the circuit with BC. The primary and secondary side of the circuit is coupled with L1 and L2 with C1 and C2, respectively. The operation of the converter is controlled by using MPWM in [22]. The following assumptions are considered to understand the operating principle of the proposed converter. 1) All active and passive devices consisting of transformer, dc source, switches, diodes, and capacitors are ideal including internal switch diode and capacitance. 2) Electrical series resistance of inductor and interwinding capacitance of transformer are neglected. 3) Voltage divider capacitors (Ca = Ca1 = Ca2) and CF are large enough to maintain constant voltage at input and output terminals of the converter. 4) The effects of the magnetizing inductance of TA are neglected.

A. Operation of Proposed Converter

The operating principle of the proposed topology in steady state is divided into eight modes (modes I–VIII) as shown in Fig. 2 and the operating waveforms are shown in Fig. 3. 1) Mode I (t0 ≤ t < t1), Fig. 2(a): Before time instant t0, lagging current (IL1 + ILA) is flowing from D1 and S2, Therefore, att0 instant, the switch S1 is turned ON with ZVS. Furthermore, a potential difference between AC and CB is created and current ILA start rising from ILA(t0) iLA = |VCa1 − VCa2 | 2LA TON −iLA(t0) |VCa1 − VCa2 | = 0 || iLA = 0) | | | | (| | | |) If → RON(S1−S4)

= 0 If → RON(S1−S4) = 0 . (1) 2) Mode II (t1 ≤ t < t2), Fig. 2(b) and (c): Before t0, switch S1 is conducting and switch current difference (iS1 − iS2) is flowing from TA (ITA1 + ITA2 = ILA). Applying KCL at points A and B and using low energy conservation iCS1 + iCS4 = iTA2 + iL1 (2) 2iCS1 = iL1 + iLA 2 . (3) At the starting of this mode, S1 is turned OFF when S3, S4 are already OFF, and S2 is still conducting. The dominant inductance L1 is now in cutoff from dc power source, and IL1 + ILA 2 starts charging switch peracetic capacitor CS1. At instant t11, VCS1 reaches VDC . After t11, IL1 finds a path by forcing the change in ILA . The inductor LA rejects this change and a current starts from S2 to S4, which discharges CS4. After CS4 voltage reaches zero, D4 turns ON and this freewheeling results in the decrement of IS2 to zero or ZCS for switch S2 t (VCS1=VDC) = 1 2CS3VDC − iL1(t1−) + iLA(t1−) 2 iL1(t) + iLA(t) 2 . (4) 3) Mode III (t2 ≤ t < t3), Fig. 2(d) and (e): This mode starts from S2 ZCS turn OFF while other switches are already OFF. During this mode, the peracetic capacitor CS2 starts charging till t21 up to VDC and the current ILA decrementing toward zero after attaining its positive peak. After t21, the current IL1 + ILA 2 finds its path by discharging capacitors CS3, CS4 and turns ON the diodes D2, D4 t1 > 2CS1 VDC iL1(t0) + iLA(t0) 2 . (5) The voltage stress across switch is given by the following expression: vS1 = VDC + vC1 (6) vS4 = −vC1 . (7) 4) Mode IV (t3 ≤ t < t4), Fig. 2(f): In this mode of operation, S4 is turned ON with ZVS as D4 is on and the voltage across S4 is near zero. The auxiliary inductor current ILA is increasing linearly in a positive direction after attaining its negative peak. 5) Mode V (t4 ≤ t < t5), Fig. 2(g): In this mode, S3 is turned ON with ZVS. IAB starts following the sinusoidal wave shape, and voltage across S3, S4 are zero as its path got completed. 6) Mode VI (t5 ≤ t < t6), Fig. 2(h) and (i): This mode starts by turning OFF S3, which triggers CS3 charging up to VDC att51. The auxiliary inductor current ILA is decreasing after attaining its peak and IL1 , ILA forces IS4 to reduce for ZCS turn-OFF condition.

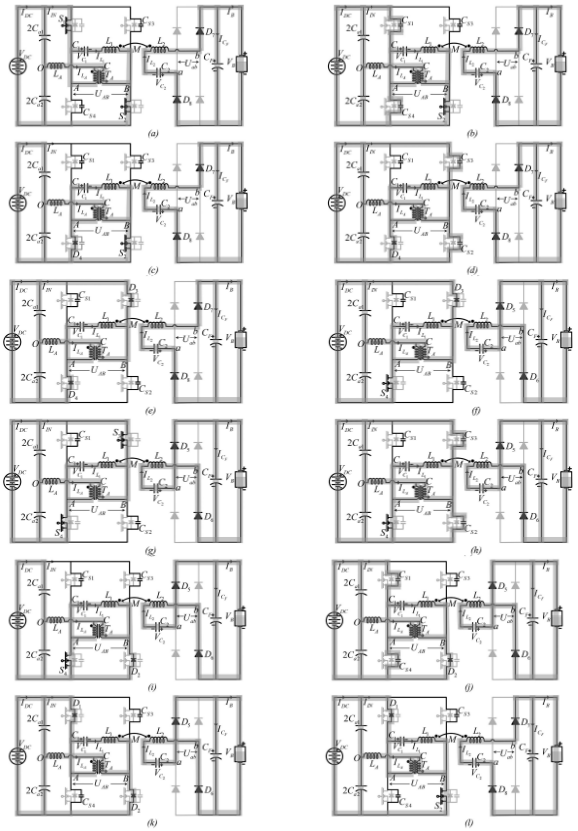

Fig. 2. Operating modes of proposed battery charger topology. (a) Mode I (t0 ≤ t < t1). (b) Mode II (part-1)

(t1 ≤ t < t11). (c) Mode II (part-2) (t11 ≤ t < t2). (d) Mode III (part-1) (t2 ≤ t < t21). (e) Mode III (part-2) (t21 ≤ t < t3). (f) Mode IV (t3 ≤ t < t4). (g) Mode V (t4 ≤ t < t5). (h) Mode VI (part-1) (t5 ≤ t < t51). (i) Mode VI (part-2) (t51 ≤ t < t6). (j) Mode VII (part-1) (t6 ≤ t < t61). (k) Mode VII (part-2) (t61 ≤ t < t7). (l) Mode VIII (t7 ≤ t < t8).

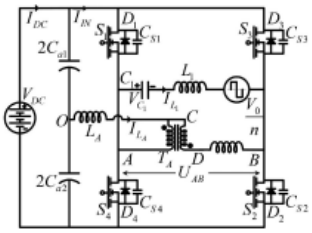

Fig. 4. Simplified network with battery load refereed at transmitter coil side.

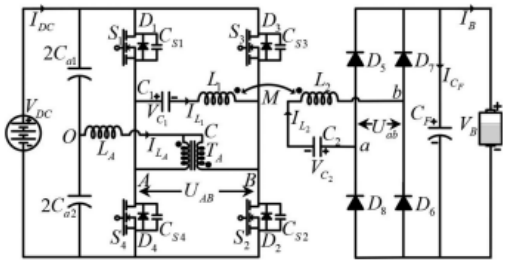

Fig. 5. Proposed network configuration of EV battery charger.

7) Mode VII (t6 ≤ t < t7), Fig. 2(j) and (k): In this mode, S4 turned OFF at ZCS and VCS4 rises up to VDC att61. Aftert61, ILA starts incriminating in positive direction. The diodes D1 and D2 turned ON and power is feedback to the source.

8) Mode VIII (t7 ≤ t < t8), Fig. 2(l): During this mode of operation, switch S2 is turned ON with ZVS and current shifts from D2 to S2. During mode, I to VIII constant voltage and current are maintained in the battery.

V.RESULTS AND DISCUSSION

The working principle of the proposed converter topology is validated by performing modeling, simulation, and hardware testing. The circuit parameters in simulation and hardware are tuned to an operating point to understand the behavior of the converter. A. Simulation Results The simulation of a proposed topology has been done in MATLAB/Simulink by using principal components, as shown Fig. 10. ZVS turn-ON for S1 − S4. in Fig. 4 and Table I. The ideal dc source is placed in series with resistor (nΩ) and inductor (nH). MOSFET switches from SimPowerSystem Library with 0 Ω resistance and 870 pF capacitance as snubber have been used to simulate H-bridge part of dc–dc converter. The auxiliary transformer is contracted by linear transformer and transmitter, receiver coils from mutual inductance. Fig. 10 shows the ZVS turn-ON of switches S1 to S4, as the voltage across the switch reaches to zero, the gate pulse is given to that particular switch to turn it ON. In Fig. 11(a) and (b), the ZCS turn-ON for switches S2 and S4 is indicated. The current from the switch becomes zero before the gate pulse finishes. Therefore it is said that the proposed wireless converter maintains ZCZVS. The compensation capacitor voltage peak value is selected by observing the performance of VC1 , as shown in Fig. 12. In Fig. 13, the input side characteristic of the primary network has been shown. These results show the small value of input dc-link capacitors does not affect the performance of the converter. The performance of the converter for BC is shown in Fig. 14(a)–(d). It is seen from Fig. 14(a) and (b) that the disturbance is very less, whereas the conventional charger having disturbance in BC voltage and current, which reduces the life of the battery and degrades the charger efficiency, whereas the nature of battery voltage and current shown in Fig. 14(c) and (d) is without using the auxiliary circuit. The circuit performance provides 93.5% efficiency with parameters.

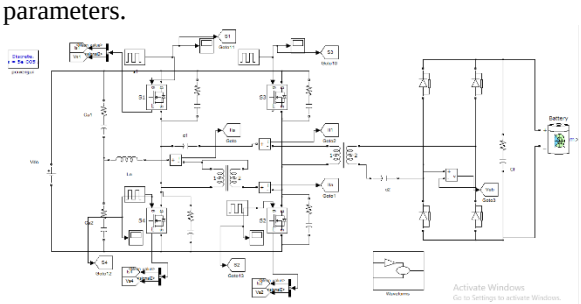

Fig: Proposed Simulation Diagram

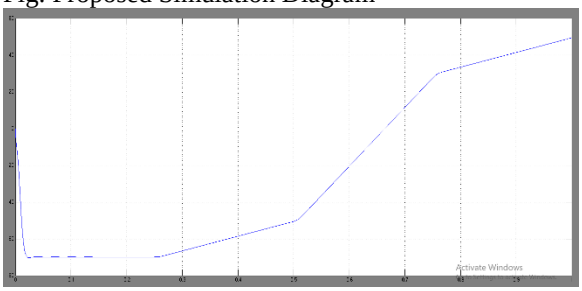

Fig: Il1

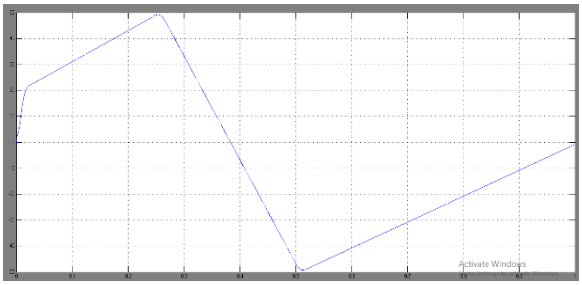

Fig: Ila

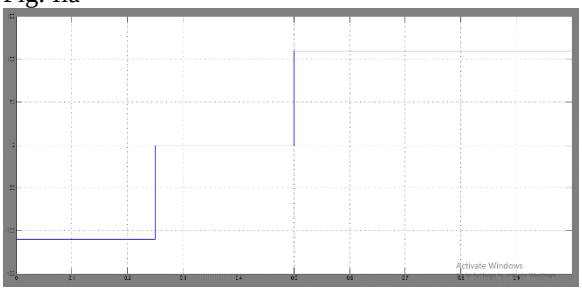

Fig: Vab

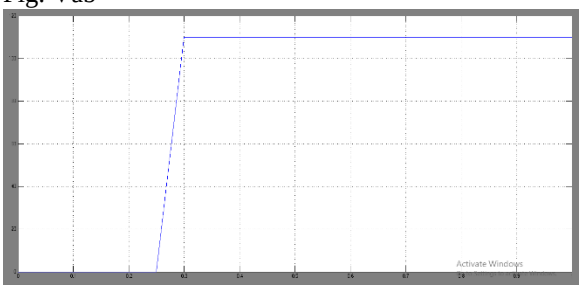

Fig: Vs1

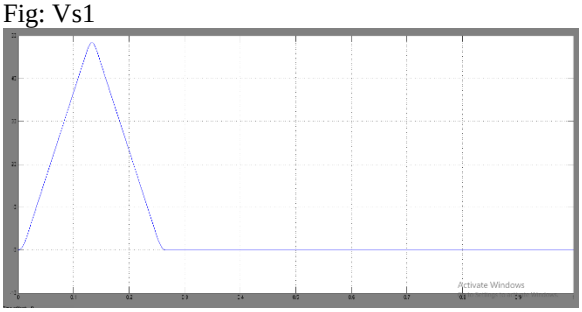

Fig: Is1

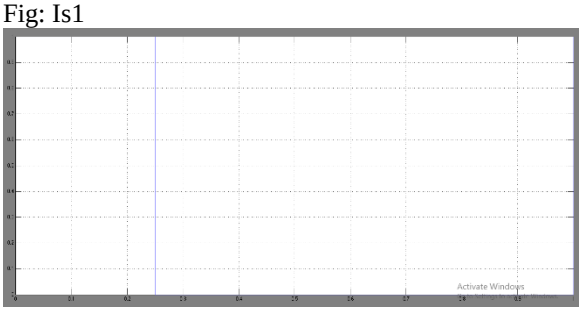

Fig: S1

CONCLUSION

In this article, the voltage fed series compensation based ZVZCS topology and its tuning method for wireless electrical vehicle battery charger have been proposed. Suitable modifications were presented for the full-bridge dc–dc converter, and enhanced performance with a wide range of input variation is achieved. The need for a high-power processor is eliminated, which further reduces the overall cost. The theoretical analysis and modeling have been presented to obtain ZVZCS with reduced control complexity. The simulation results verified the ZVZCS condition of the proposed topology for a full load range. The offered solution produced less ripple in input/ output voltage and current while utilizing a low value of dc link, and filter capacitance values, respectively. An acceptable efficiency of 91.26% has been achieved for both battery and resistive loads.

REFERENCES

[1] M. Granovskii, I. Dincer, and M. A. Rosen, “Economic and environmental comparison of conventional, hybrid, electric and hydrogen fuel cell vehicles,” J. Power Sources, vol. 159, no. 2, pp. 1186–1193, 2006.

[2] S. B. Peterson, J. Whitacre, and J. Apt, “The economics of using plug-in hybrid electric vehicle battery packs for grid storage,” J. Power Sources, vol. 195, no. 8, pp. 2377–2384, 2010.

[3] Y. Zhou, M. Wang, H. Hao, L. Johnson, and H. Wang, “Plug-in electric vehicle market penetration and incentives: A global review,” Mitigation Adaptation Strategies Global Change, vol. 20, no. 5, pp. 777–795, 2015.

[4] B. Nykvist and M. Nilsson, “Rapidly falling costs of battery packs for electric vehicles,” Nature Climate Change, vol. 5, no. 4, pp. 329–332, 2015.

[5] W. Zhang and C. C. Mi, “Compensation topologies of high-power wireless power transfer systems,” IEEE Trans. Veh. Technol., vol. 65, no. 6, pp. 4768–4778, Jun. 2016.

[6] K. Mude and K. Aditya, “Comprehensive review and analysis of two-element resonant compensation topologies for wireless inductive power transfer systems,” Chin. J. Elect. Eng., vol. 5, no. 2, pp. 14–31, 2019.

[7] Y. Jiang, L. Wang, Y. Wang, J. Liu, X. Li, and G. Ning, “Analysis, design, and implementation of accurate ZVS angle control for EV battery charging in wireless high-power transfer,” IEEE Trans. Ind. Electron., vol. 66, no. 5, pp. 4075–4085, May 2019.

[8] Y. Jiang, L. Wang, Y. Wang, J. Liu, M. Wu, and G. Ning, “Analysis, design, and implementation of WPT system for EV’s battery charging based on optimal operation frequency range,” IEEE Trans. Power Electron., vol. 34, no. 7, pp. 6890–6905, Jul. 2019.

[9] D. H. Tran, V. B. Vu, and W. Choi, “Design of a high-efficiency wireless power transfer system with intermediate coils for the on-board

chargers of electric vehicles," IEEE Trans. Power Electron., vol. 33, no. 1, pp. 175–187, Jan. 2018.

[10] S. Moon and G.-W. Moon, "Wireless power transfer system with an asymmetric four-coil resonator for electric vehicle battery chargers," IEEE Trans. Power Electron., vol. 31, no. 10, pp. 6844–6854, Oct. 2016.